Acta Crystallographica Section B
Structural Science
ISSN 0108-7681

Symmetry and twins in the monophosphate tungsten bronze series $(PO_2)_4(WO_3)_{2m}$ ($2 \leq m \leq 14$)

Pascal Roussel,* Philippe Labbé and Daniel Groult

Laboratoire CRISMAT, CNRS UMR 6508, ISMRA-Université de Caen, 14050 Caen CEDEX, France

Correspondence e-mail: pascal.roussel@ismra.fr

Received 23 August 1999
Accepted 9 December 1999

Monophosphate tungsten bronze with pentagonal tunnels $(PO_2)_4(WO_3)_{2m}$ are low-dimensional materials with charge density wave (CDW)-type electron instabilities. Two forms of the structure can thus be expected for all the members of the series: a low-temperature form (LT) corresponding to the CDW state and a high-temperature form (HT) corresponding to a normal metallic state. The HT form is described here for m = 9 and compared with that of the m = 5 and m = 7 counterparts. It is shown that a systematic twin phenomenon must be taken into account for HT members because of two possible configurations of the tilting mode of WO_6 octahedra. The structure is also compared with that of m = 10, which exhibits the modulated CDW–LT form at room temperature. Owing to two possible polarization directions of the segments built of m WO_6 octahedra, a twin phenomenon is also encountered in the LT forms. A review of all the structures known at present (m = 2, 4, 5, 6, 7, 8, 9, 10, 12) leads us to propose a structural law based on the building mode of WO_6 octahedra in WO_3-type slabs to explain the symmetry changes observed between even and odd members of the series.

1. Introduction

The first crystal of the monophosphate tungsten bronze family with pentagonal tunnels (MPTBp) was synthesized more than 18 years ago (Giroult *et al.*, 1981). It appeared afterwards that this class of oxide provides, after those of molybdenum, an interesting model of quasi two-dimensional metallic conductors (Schlenker, 1989; Schlenker, Dumas *et al.*, 1996). These compounds show, as a function of temperature, phase transitions, called Peierls transitions, towards a state in which a charge density wave (CDW) is established. The physical interpretation of these electronic instabilities implies, within a framework of a low-dimensional system, both nesting properties of the Fermi surface and electron–phonon type coupling effects (Whangbo *et al.*, 1991; Foury, 1993). At the Peierls temperature (T_p), only a part of the Fermi surface is destroyed, involving a metal-to-metal transition. Below T_p, the CDW state is due to a coupling between the lattice and the electron density, condensed through a modulation phenomenon (for a review see Greenblatt, 1993).

As for the copper-based high-temperature superconducting oxides, which are also quasi two-dimensional metals, the crystal structure of the MPTBp members is a layered structure, and the mechanisms which control the occurrence of either the superconducting or the CDW instabilities have been studied in this context. For the monophosphate tungsten bronzes, various aspects of the physical properties have been investigated such as X-ray diffuse scattering, spectroscopic

characteristics, transport features (electrical resistivity, thermopower, Hall effect, magnetoresistance and magnetotransport), thermodynamic properties and electron band filling, referring to an extremely large variety of physical phenomena (for a review see Schlenker, Dumas *et al.*, 1996).

The quasi two-dimensional character of the monophosphate tungsten bronzes with pentagonal tunnels (MPTBp) is closely related to their crystal structures. It is usual, indeed, to describe the atomic arrangement of these oxides $(PO_2)_4(WO_3)_{2m}$ as a stacking of WO_3-type layers whose thickness is characterized by m values. These layers cut parallel to $\{211\}p$ (p for perovskite axes), infinite in two directions, and are separated by slices of isolated phosphate groups (Fig. 1). This feature is generated by the fact that, in a 'perovskite cage' bound by eight WO_6 octahedra sharing corners, a PO_4 tetrahedron can replace a WO_6 octahedron. This causes a slight local distortion since the O—O distance in a PO_4 tetrahedron is about 2.5 Å whereas it is 2.7 Å in a WO_6 octahedron (Fig. 2). However, the comparison with the WO_3 structure shows mostly differences. They are related, in particular, to the distortion between the O—O distances on the sides of the slabs, to the tilting mode of the polyhedra and to the oxygen neighbourhood of W atoms, which varies from one W atom to the next, involving a particular distribution of the electronic density within the slabs. At the junction between two slabs, one can observe cages bounded with 18 O atoms. These O_{18} cages are connected through windows which have a pentagonal shape and can appear as tunnels in some directions, hence the name given to the different members of the series. Note that generally the O_{18} cages are empty, and most of the samples crystallize in this way. For a long time we believed that the insertion of cations into this matrix was impossible and that the crystallization of doped compounds always led to members of another family: the so-called monophosphate tungsten bronzes with hexagonal tunnels (MPTBh) $A_x(PO_2)_4(WO_3)_{2m}$ (A = Na, K, Pb), which also enclose analogous O_{18} cages. In fact, as proved recently, it has been possible to synthesize MPTBp members ($m \geq 6$) with Na^+ as inserted cations ($0 \leq x \leq 1$; Roussel, Groult *et al.*, 1999). However, if the electronic configuration may be modified, it has been verified that the steric influence of the inserted cation upon the atomic polyhedral arrangement is negligible.

The present paper deals with the crystallographic features of the MPTBp family $(PO_2)_4(WO_3)_{2m}$. The crystal data of the different members of this family are now known just as well from X-ray determinations and electron-microscope investigations as from the diffuse scattering observations. Moreover, some members have structural molybdenum counterparts with which the comparison is instructive. This suggests to attempt a synthesis relative to the symmetry found in these crystals and to the twin phenomenon often encountered in these phases, in relation to their structural features.

2. Survey of the WO_3 structure

In the MPTBp series with the formula $(PO_2)_4(WO_3)_{2m}$ the thickness of the WO_3-type slabs increases with the m value. For high values of m it is reasonable to assume that the structure of the slabs tends to be that of WO_3, despite the geometrical influence of the PO_4 tetrahedra located on each side of the slabs. Apparently very simple, the structure of this oxide is, however, wealthy from the crystal symmetry point of view. One indeed observes five varieties of WO_3 according to temperature. Recently, comprehensive studies have been performed with high-resolution neutron diffraction and the structural aspects of this compound have been revisited (Fig. 3): α-WO_3 (Kehl *et al.*, 1952; Vogt *et al.*, 1999); β-WO_3 (Salje, 1977; Vogt *et al.*, 1999); γ-WO_3 (Loopstra & Rietveld, 1969; Woodward *et al.*, 1995); δ-WO_3 (Diehl *et al.*, 1978; Woodward *et al.*, 1995); ε-WO_3 (Woodward *et al.*, 1997). The five forms have very similar structures consisting of tridimensional networks of corner-sharing WO_6 octahedra, always described with respect to the ideal cubic structure of ReO_3-type, chosen as a reference. [The cubic phase of pure WO_3 does not exist without inserted cations, but is stabilized with Na located in the perovskite cages (Magnéli, 1949).]

The tilting of the octahedra is a general phenomenon for the five WO_3 structures and can be described as the result of the octahedral rotation about the Cartesian axes (perovskite axes) from their ideal orientation. The value of this angle is roughly the same for all tilting, about 8°; however, the rotation may be

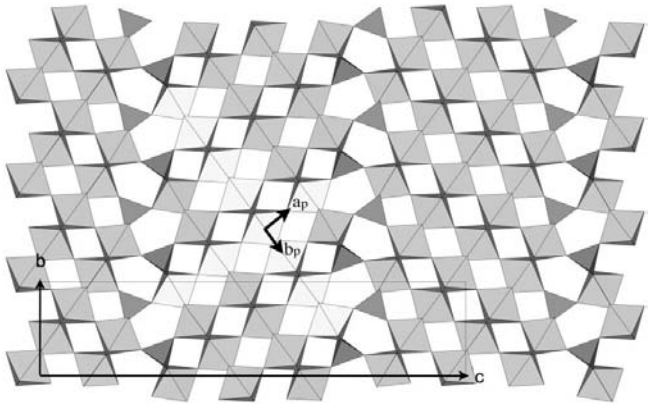

Figure 1
Structure of the $m = 8$ member ($P_4W_{16}O_{56}$) viewed along [100]. The three axes of the octahedra, $\mathbf{a}_p$, $\mathbf{b}_p$ and $\mathbf{c}_p$ (p index referring to the perovskite axes), are indicated.

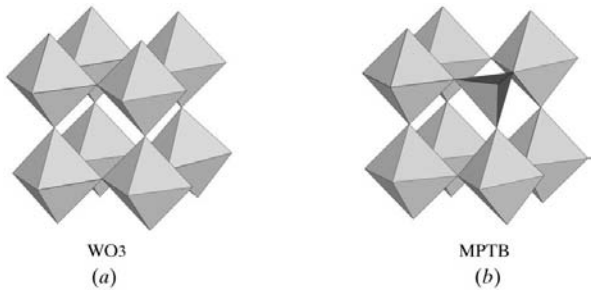

Figure 2
Replacement of one WO_6 octahedron in a structure of ReO_3-type. (*a*) Classical perovskite cage; (*b*) one WO_6 octahedron is substituted for a PO_4 tetrahedron leading to the monophosphate tungsten bronze family.

clockwise or anticlockwise. According to Glazer (1972) the easiest way to observe the tilt system is to view a polyhedral representation of the structure down to each of the three directions of the perovskite along which the octahedra share corners, giving the +, − and 0 symbols for the in-phase, out of phase and absence of tilting, respectively, about each of the Cartesian axes. One notices in Fig. 3 that, for the five structures, tilts are present in at least one direction (the ideal cubic structure, without tilting, is given as a reference). One can note three types of behaviour for the WO_6 octahedra. Along the [100] and [010] directions of the α-form, as well as along the [100] direction of the β-phase, there is no tilting of the WO_6 octahedra, the perovskite windows being square-shaped. Along the [010] direction of β- and γ-WO_3, one observes in-phase tilting and, consequently, looking down this direction the diamond-shaped windows are superimposed. In all the other directions, tilts are present but are out of phase from one layer to the other. The tilt system is then, using the Glazer notation, $(a^-b^-c^-)$ for ε- and δ-WO_3, $(a^-b^+c^-)$ for γ-WO_3, $(a^0b^+c^-)$ for β-WO_3 and finally $(a^0b^0c^-)$ for the α variety.

One can now apply this reasoning to the WO_3-type slabs of the monophosphate tungsten bronze with pentagonal tunnels and for instance on $P_4W_{16}O_{56}$, the $m = 8$ member of the series (Fig. 1). Let us refer to one octahedral slab as a set of three perovskite axes, $\mathbf{a}_p$, $\mathbf{b}_p$ and $\mathbf{c}_p$, parallel to the octahedral axes, $\mathbf{a}_p$, running along the apical axis of a segment defined by four octahedra, $\mathbf{b}_p$ and $\mathbf{c}_p$ being in the perpendicular plane. The projections of the structure along these three directions show (Fig. 4) that along $\mathbf{a}_p$ all the tilts are in-phase and the aspect of the diamond-shaped windows is maintained. On the contrary, down to the other two directions $\mathbf{b}_p$ and $\mathbf{c}_p$, which include segments of eight WO_6 octahedra, there is no tilt phenomenon and the octahedra appear as in the ideal reference ReO_3 structure, thereby involving in these directions windows of the perovskite cages with almost square shapes. Therefore, the tilt system in $P_4W_{16}O_{56}$ and in all the MPTBp series is $(a^+b^0c^0)$, indicating that there is an in-phase tilting along $\mathbf{a}_p$, whereas no tilting is found along $\mathbf{b}_p$ and $\mathbf{c}_p$. In this respect the tilting mode observed in all the members of the series including those with the highest m values are distinct from all those found for the different forms of pure WO_3.

This tilting phenomenon of the WO_6 octahedra leads to many structural characteristics. As we will see later, in this way one can explain the different symmetries observed in the series according to the parity of m, as well as the appearance of twinning phenomena.

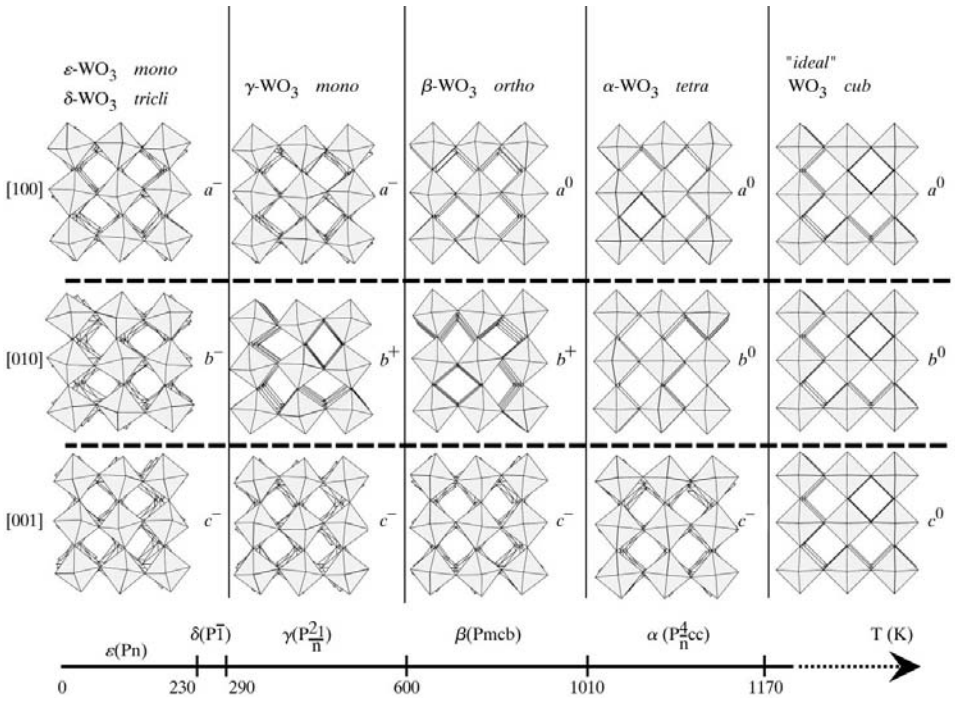

Figure 3
Tilt patterns and stability temperature domains of the different polymorphs of WO_3 (Woodward *et al.*, 1997).

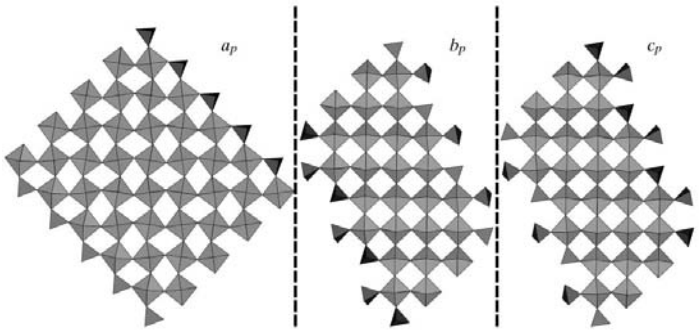

Figure 4
WO_6 octahedral tilting in the MPTBp series. Note that tilting of the WO_3 framework occurs only about the $\mathbf{a}_p$ direction.

3. The MPTBp family

Table 1 collects information available at present on the different members $(PO_2)_4(WO_3)_{2m}$ of the MPTBp family, up to $m = 14$, relative to their structural properties. Most of them have been published in the past, and some of them will be published in the near future. In addition, the references of the physical properties are given. One

Table 1
Summary of crystallographic properties for the series MPTBp.

m	Formula	Symmetry and space group at RT	Cell parameters	Twin plane	T_p (K)	Modulation wavevector $\mathbf{q}_p^{(m)}$ (reciprocal lattice units)	Physical properties	Structural properties
2	$P_4W_4O_{20}$	Monoclinic, SG: ?	a = 5.22 Å, b = 6.54 Å, c = 11.17 Å, α = 90.34°				Teweldemedhin *et al.* (1991)	Kinomura *et al.* (1988)
2†	$P_4W_4O_{20}$	Orthorhombic, SG: $P2_1cn$	a = 5.23 Å, b = 6.55 Å, c = 11.17 Å					Wang, Wang & Lii (1989)
3								
4†	$P_4W_8O_{32}$	Orthorhombic, SG: $P2_12_12_1$	a = 5.28 Å, b = 6.57 Å, c = 17.35 Å		80 (±1), 52 (±1)	$\mathbf{q}_1^{(4)}$ = [0.330 (5), 0.295 (5), ?], $\mathbf{q}_2^{(4)}$ = [0.340 (5), 0.000 (5), ?]	Teweldemedhin *et al.* (1992); Lehmann *et al.* (1993); Rötger *et al.* (1993, 1994); Le Touze *et al.* (1995); Schlenker *et al.* (1995); Hess *et al.* (1996); Schlenker, Hess *et al.* (1996)	Giroult *et al.* (1981); Domengès *et al.* (1984); Foury & Pouget (1993); Foury, Pouget, Teweldemedhin, Wang & Greenblatt (1993); Foury, Pouget, Teweldemedhin, Wang, Greenblatt & Groult (1993); Ludecke *et al.* (2000)
5†	$P_4W_{10}O_{38}$	Monoclinic, SG: $P2_1/n$	a = 5.28 Å, b = 6.57 Å, c = 20.45 Å, β = 90.40°	(001)	83 (±5), 60 (±2)	$\mathbf{q}_1^{(4)}$ = [0.32 (1), 0.29 (1), 0.0 (1)], $\mathbf{q}_2^{(4)}$ = [0.36 (1), 0.00 (5), 0.0 (1)]	Beierlein *et al.* (1999)	Foury *et al.* (1999); Roussel, Foury *et al.* (1999)
5† (4+6)	$P_4W_{10}O_{38}$	Monoclinic, SG: $P2_1$	a = 5.28 Å, b = 6.57 Å, c = 20.57 Å, α = 96.18°		158 (±2), ?	$\mathbf{q}_1^{(4)}$ = [0.330 (5), 0.295 (5), ?], $\mathbf{q}_2^{(4)}$ = [0.33 (4), 0.00 (4), ?]	Schlenker, Hess *et al.* (1996); Hess, Le Touze, Schlenker, Dumas & Groult (1997)	Benmoussa *et al.* (1982); Domengès *et al.* (1984); Foury *et al.* (1999); Roussel, Foury *et al.* (1999)
6†	$P_4W_{12}O_{44}$	Orthorhombic, SG: $P2_12_12_1$	a = 5.29 Å, b = 6.56 Å, c = 23.55 Å		120 (±1), 62 (±1), ∼30	$\mathbf{q}_1^{(6)}$ = [0.385 (5), 0.000 (5), ?], $\mathbf{q}_2^{(6)}$ = [0.310 (5), 0.295 (5), ?], $\mathbf{q}_3^{(6)}$ = [0.29 (2), 0.11 (2), ?]	Wang, Greenblatt *et al.* (1989); Lehmann *et al.* (1993); Rötger *et al.* (1993, 1994); Le Touze *et al.* (1995); Hess *et al.* (1996); Schlenker, Hess *et al.* (1996); Witkowski *et al.* (1997)	Domengès *et al.* (1984); Labbé *et al.* (1986); Foury *et al.* (1991, 1992); Foury & Pouget (1993); Foury, Pouget, Teweldemedhin, Wang & Greenblatt (1993); Foury, Pouget, Teweldemedhin, Wang, Greenblatt & Groult (1993)
7†	$P_4W_{14}O_{50}$	Monoclinic, SG: $P2_1/n$	a = 5.29 Å, b = 6.56 Å, c = 26.65 Å, β = 90.19°	(001)	188 (±1), 60 (±1)	$n\mathbf{q}_1^{(7)} = n$[0.260 (3), 0.073 (3), 0.27 (5)], n = 1, 2, 3, 4, 5, 6, 7; $n\mathbf{q}_2^{(7)} = n$[0.12 (1), 0.03 (1), 0.15 (5)], n = 1, 3, 5	Lehmann *et al.* (1993); Rötger *et al.* (1993, 1994); Schlenker, Hess *et al.* (1996); Hess, Schlenker, Bonfait, Marcus *et al.* (1997); Hess, Schlenker, Bonfait, Ohm *et al.* (1997); Hess (1997)	Domengès *et al.* (1984); Foury *et al.* (1992); Foury & Pouget (1993); Foury, Pouget, Teweldemedhin, Wang & Greenblatt (1993); Foury, Pouget, Teweldemedhin, Wang, Greenblatt & Groult (1993); Domengès *et al.* (1996); Roussel *et al.* (1996)
8†	$P_4W_{16}O_{56}$	Orthorhombic, SG: $P2_12_12_1$	a = 5.29 Å, b = 6.55 Å, c = 29.70 Å		∼220, ∼ 200	SRO: $\mathbf{q}_1^{(8)}$ = [0.47 (2), 0.02 (1), 0.15 (10)], SRO: $n\mathbf{q}_2^{(8)} = n$[0.19 (2), 0.03 (1), 0.15 (5)], n = 1, 2, 3, 4, 5, 6	Schlenker, Hess *et al.* (1996); Witkowski *et al.* (1997); Hess, Le Touze, Schlenker, Dumas, Groult & Marcus (1997); Hess (1997)	Domengès *et al.* (1984); Labbé *et al.* (1986); Ottolenghi *et al.* (1995); Ottolenghi & Pouget (1996)

Table 1 (continued)

m	Formula	Symmetry and space group at RT	Cell parameters	Twin plane	T_p (K)	Modulation wavevector $\mathbf{q}_p^{(m)}$ (reciprocal lattice units)	Physical properties	Structural properties
9†	$P_4W_{18}O_{62}$	Triclinic, SG: $P\bar{1}$	a = 5.29 Å, b = 6.54 Å, c = 32.74 Å, α = 90.00°, β = 90.20°, γ = 89.78°	(001)		No satellites at room temperature		Domengès *et al.* (1984); this work
9	$P_4W_{18}O_{62}$				565 (±5), 330 (±5)	$\mathbf{q}_0^{(9)}$ = [0.50 (1), 0.00 (1), 0.0 (2)], $\mathbf{q}_1^{(9)}$ = [0.17 (1), 0.00 (1), 0.0 (2)]	Schlenker, Hess *et al.* (1996); Hess, Le Touze, Schlenker, Dumas, Groult & Marcus (1997); Witkowski *et al.* (1997); Hess (1997)	Foury, Pouget, Teweldemedhin, Wang, Greenblatt & Groult (1993); Ottolenghi *et al.* (1995); Ottolenghi & Pouget (1996)
10†	$P_4W_{20}O_{68}$	Monoclinic, SSG: $P{:}P2_1(\bar{1})$	a = 5.30 Å, b = 6.55 Å, c = 35.82 Å, γ = 90.60°	(100)	∼450	$\mathbf{q}^{(10)}$ (300 K) = [0.43 (1), 0.00 (1), 0.0 (1)], $\bar{\mathbf{q}}^{(10)}$ (300 K) = [0.14 (1), 0.00 (1), 0.0 (1)]	Schlenker *et al.* (1995); Witkowski *et al.* (1997)	Foury, Pouget, Teweldemedhin, Wang, Greenblatt & Groult (1993); Ottolenghi *et al.* (1995); Ottolenghi & Pouget (1996); Roussel *et al.* (2000)
11	$P_4W_{22}O_{72}$				560 (±5)	$n\mathbf{q}^{(11)}(T)$, n = 1, 2, 3; $\mathbf{q}^{(11)}$ (300 K) = [0.43 (1), 0.00 (1), 0.0 (1)]		Domengès *et al.* (1984); Foury, Pouget, Teweldemedhin, Wang, Greenblatt & Groult (1993); Ottolenghi & Pouget (1996); Roussel, Labbé & Groult (1999)
12†	$P_4W_{24}O_{80}$	Orthorhombic, SG: $P2_12_12_1$	a = 5.31 Å, b = 6.55 Å, c = 42.11 Å			No satellites at room temperature		Domengès *et al.* (1984); Roussel *et al.* (1998)
12	$P_4W_{24}O_{80}$	Monoclinic, SSG: ?	a = 5.31 Å, b = 6.55 Å, c = 42.00 Å, γ = 90.72°	(100)	535 (±5), 500 (±5)	$\mathbf{q}_1^{(12)}$ = [0.12 (1), 0.00 (2), 0.0 (2)], $\mathbf{q}_0^{(12)}$ = [0.50 (1), 0.00 (1), 0.5 (2)]	Schlenker *et al.* (1995); Schlenker, Hess *et al.* (1996); Witkowski *et al.* (1997); Hess, Le Touze, Schlenker, Dumas, Groult & Marcus (1997)	Yan *et al.* (1995); Ottolenghi & Pouget (1996); Roussel, Labbé & Groult (1999)
13	$P_4W_{26}O_{86}$	Monoclinic, SG: ?	a = 5.32 Å, b = 6.55 Å, c = 45.04 Å, γ = 91.06°	Yes?	550 (±5), 510 (±5), 160 (±10)	$n\mathbf{q}_1^{(13)}$ = [0.053 (8), 0.016 (10), ?], n = 1, 2; $\mathbf{q}_0^{(13)}$ = [0.50 (1), 0.00 (1), 0.0 (2)], $\mathbf{q}_2^{(13)}$ = [0.178 (8), 0.145 (10), ?]	Schlenker, Hess *et al.* (1996); Hess, Le Touze, Schlenker, Dumas, Groult & Marcus (1997); Hess, Schlenker, Hodeau *et al.* (1997)	Ottolenghi & Pouget (1996); Hess, Schlenker, Hodeau *et al.* (1997); Favre-Nicolin & Hodeau (1998)
14	$P_4W_{28}O_{92}$	Monoclinic, SSG: $A{:}P2_1/n(1\bar{1})$	a = 5.32 Å, b = 6.54 Å, c = 48.00 Å, γ = 91.04°	(100)	730/695	$\mathbf{q}_0^{(14)}$ = [0.50 (1), 0.00 (1), 0.5 (2)]	Schlenker, Hess *et al.* (1996); Hess, Le Touze, Schlenker, Dumas, Groult & Marcus (1997)	Domengès *et al.* (1984); Ottolenghi & Pouget (1996); Roussel, Labbé & Groult (1999)

† Solved from single-crystal X-ray data.

must keep in mind that the structural building is exactly the same for all the members of the series: their layered crystal structure is made of the regular stacking of parallel slabs of WO_3-type interconnected through isolated PO_4 tetrahedra. The successive slabs, built up of WO_6 octahedral sharing corners, are in general of the same thickness which depends upon the m value. As previously noticed, within a slab, the comparison with the WO_3 structure is helpful because it allows one to identify more easily along the reference perovskite axes the three directions of the linear octahedra chains, hereafter segments, since they are limited at each end by PO_4 tetrahedra. The shortest segment includes $m/2$ octahedra for even m (Fig. 5*a*), $(m + 1)/2$ and $(m - 1)/2$ octahedra for odd m (Fig. 5*b*); the other two segments always include m WO_6

octahedra whatever the parity of m (see Fig. 6*a* for an even m member and Fig. 6*b* for an odd one). Analogous chains could be gathered in octahedral slices, one octahedron high, parallel to basic perovskite planes and edged with PO_4 tetrahedra. If, on one hand, the two parameters **a** and **b** of the lattices, located in the plane of the slabs, are always of the same order, $\mathbf{a} \simeq 5.3$, $\mathbf{b} \simeq 6.6$ Å, because they are related to the classical $\mathbf{a}_p$ perovskite parameter ($\mathbf{a} \simeq \mathbf{a}_p 2^{1/2}$, $\mathbf{b} \simeq \mathbf{a}_p 3^{1/2}$); on the other hand, **c** increases linearly with m, according to the empirical relation $\mathbf{c} = m\mathbf{a}_p \cos 35^\circ + K$, where the K value is about 4.90 Å (Domengès *et al.*, 1988). The previous **a**, **b** and **c** appellations have been retained in Table 1 and afterwards for Mo counterparts, for suitable comparison, whatever m, even though their denominations were interchanged in the connected publications.

The examination of the symmetry for the different m members is somewhat a little surprising. One indeed finds, despite very similar structural models, either orthorhombic or monoclinic lattices, with **b** or **c** as the twofold axis, and also a triclinic lattice; one finds both centric and acentric symmetries. Sometimes the same m value leads to two different structures at room temperature and, at various temperatures, satellite reflections often appear in the diffraction patterns, which are an indication of a modulated structure formation. Finally, the crystallographic state became complicated because a large number of m members always appeared as twinned crystals, which led to more difficult data collections and resolutions. For $m = 3$, a classical synthesis route has led to the stabilization of a pure powder phase, $P_8W_{12}O_{52}$, and a structural study performed on a selected single crystal showed an original structure based on WO_6 octahedra and P_2O_7 diphosphate groups sharing corners (Domengès *et al.*, 1982).

According to the physical properties, and particularly to electrical conductivity and specific heat (Le Touze, 1996), the members with a low m value ($m < 7$) contrast with those with a high m value ($m > 7$). From a structural point of view it seems more interesting to separate the terms with even values of m from those with odd values. This choice is governed by the fact that all the known detailed structures of even m compounds correspond to an orthorhombic lattice, at least up to $m = 8$ and perhaps also for greater values, whereas all the members with odd m value have a monoclinic lattice.

4. The even *m* members

The detailed structure of the even m members of the MPTBp series are known up to $m = 12$. Among these six compounds (m = 2, 4, 6, 8, 10 and 12), only $P_4W_{20}O_{68}$ ($m = 10$) does not possess orthorhombic symmetry (Roussel *et al.*, 2000). However, it should be noted that $P_4W_{24}O_{80}$ ($m = 12$) crystallizes with two forms: one with a monoclinic lattice at a temperature lower than 500 K and the other one, which has been quenched at room temperature, with an orthorhombic lattice and $P2_12_12_1$ space group (Roussel *et al.*, 1998). It is also very likely that two forms also exist for $P_4W_{20}O_{68}$ ($m = 10$): a low-modulated-temperature form which is monoclinic (Roussel *et al.*, 2000) and a high-temperature form which is orthorhombic. Indeed, it has been reported (Ottolenghi, 1996)

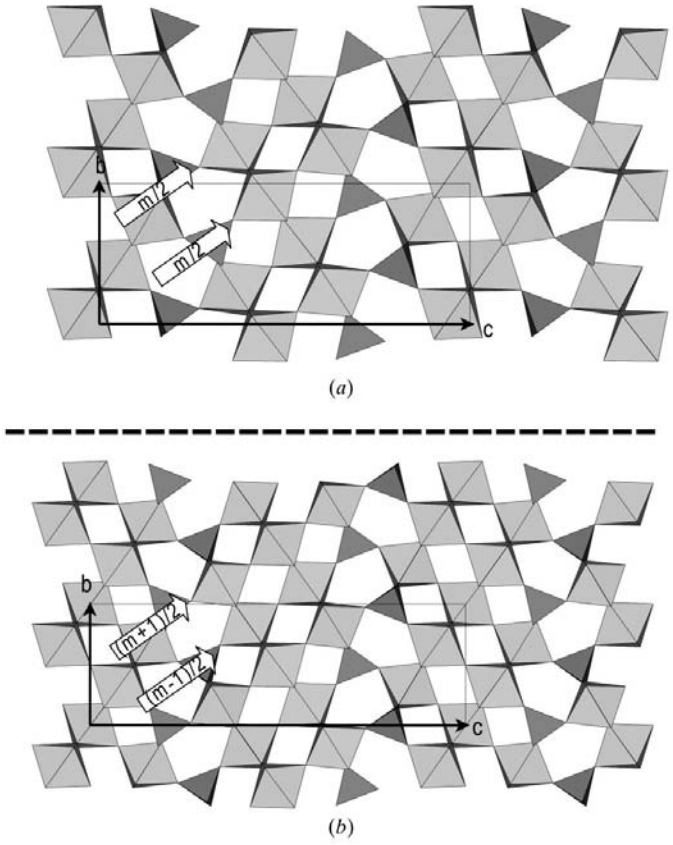

Figure 5
Projections on [100] of (*a*) the $m = 4$ member ($P_4W_8O_{32}$) and (*b*) the $m = 5$ member ($P_4W_{10}O_{38}$). On these projections, the shortest segments (represented by white arrows) include $m/2$ octahedra for even m members (*a*) whereas they are alternatively $(m + 1)/2$ and $(m - 1)/2$ long for odd m members (*b*).

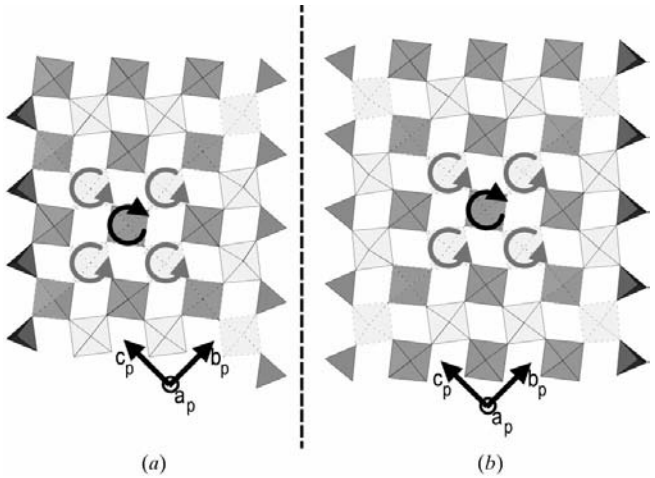

Figure 6
Projection along the $\mathbf{a}_p$ direction of (*a*) $P_4W_{12}O_{44}$ (m = 6) and (*b*) $P_4W_{14}O_{50}$ (m = 7). In this type of section, segments (delimited by PO_4 tetrahedra) always include m WO_6 octahedra, whatever the parity of m. If an octahedron is tilted clockwise, the four neighbour octahedra are rotated counterclockwise.

that by heating a monoclinic twinned crystal of $P_4W_{20}O_{68}$ at a temperature higher than T_c = 450 K, one observes that the twin effect disappears and the cell becomes orthorhombic. Therefore, one can assume that there exists, for each even *m* member of the MPTBp series, an orthorhombic high-temperature form and a low-temperature form (at $T < T_c$) which exhibits a more complex structure with distortion of the lattice and lower symmetry.

4.1. The tilting mode

As the structural building principle of all the even *m* values is the same, consisting of sets of parallel segments of *m*/2 WO_6 octahedra arranged in a chevron-type manner joined through slices of PO_4 tetrahedra, one can use a hypothetical starting model from which the actual structures are derived. Such a model (Fig. 7*a*) involves regular WO_6 octahedra and PO_4 tetrahedra. This model looks like slabs of ReO_3-type in which all the octahedra-sharing corners are oriented in the same manner. The space group corresponding to such a hypothetical atomic arrangement is $P2_1/m\ 2_1/c\ 2_1/n$ (no. 62, standard: *Pnma*). However, there is a peculiarity which applies to all the structures of the MPTBp series: one indeed observes that all the *m*/2 octahedra-sharing corners in a segment are tilted in the same sense with an angle of about 8°, whereas no tilting system is observed down to the other two reference axes of the perovskite (Fig. 4). If we consider such a segment, chosen as a reference in a given slab, and a rotation, *e.g.* clockwise, the four neighbour segments are rotated counterclockwise (Fig. 7*b*). These rotations imply a reduction of the symmetry. For example, the (*m*) mirror normal to **a** disappears; but the 2_1 screw axis parallel to **a** is maintained and we know that the resulting global group must be a subgroup of *Pmcn*, the group of the idealized structure. This subgroup is dependent on the mutual arrangement of two successive slabs of the structure along **c**. There are two different possibilities according to the relative octahedral tilting mode of one slab of WO_3-type with respect to the next one. If the (*n*) glide plane parallel to (001) is retained, one obtains the drawing (Fig. 8) with the $P2_1cn$ group, referring to **a**, **b** and **c**. This group is actually found for $P_4W_4O_{20}$ (*m* = 2; Wang, Wang & Lii, 1989) and also for γ-Mo_4O_{11} which is an MPTBp structural counterpart (Ghedira *et al.*, 1985) in which W and P are substituted by Mo. If the three mirrors are eliminated, then one obtains the $P2_12_12_1$ group with the second possible tilting mode (Fig. 9) as observed for the *m* = 4, 6, 8 and 12 members. Thus, in the example in Figs. 8 and 9, if we consider a polyhedral zigzag chain along **c** (light grey on the projections), built up of three octahedra, one tetrahedron, three octahedra, one tetrahedron *etc.*, all at the same *x* level, it is easy to perceive the difference between the two possible joint segments in two adjacent slabs since the direction of tilting is changed (*cf.* γ-Mo_4O_{11}), with a rotation about 16° of the PO_4 tetrahedra limiting the pentagonal tunnels, or the tilting is not changed as in $P_4W_{12}O_{44}$. Another approach to conceive the structure is to consider that each slab includes the PO_4 tetrahedra on each side. A PO_4 tetrahedron is then joined through three oxygen apices to three WO_6 octahedra inside a slab and with one apex free, with which it is related to the next slab. If all the octahedral segments of the next slab are tilted in the other direction, the PO_4 tetrahedron also turns but the position of the free apex is almost not affected, in such a way that the tilt mode of the neighbour slab does not matter. The remarkable fact is that these two possibilities of linkage are present and are settled down without distortion of the lattice, which remains orthorhombic without a change in the parameters.

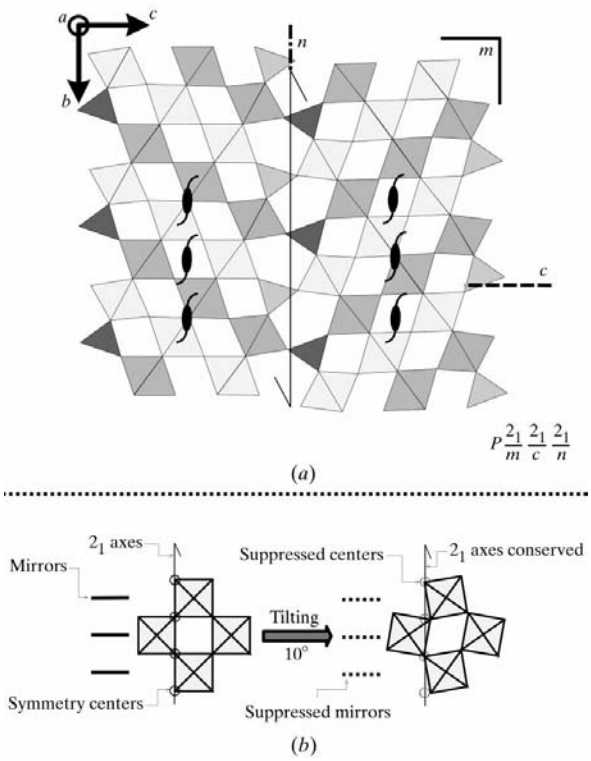

Figure 7
(*a*) Hypothetical structural model of an even *m* member of the MPTBp series (here *m* = 6) and its related space group. (*b*) Schematic representation of the WO_6 octahedra in the idealized model (left) and in the actual tilted structure (right).

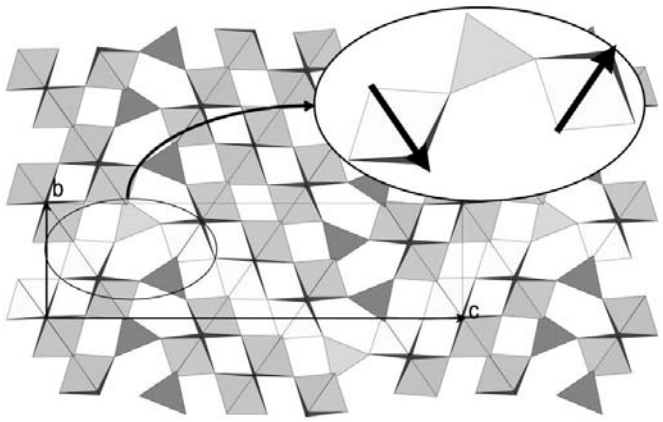

Figure 8
Tilting mode of the octahedra found in γ-Mo_4O_{11} ($P2_1cn$). Arrows are symbolic representations of the WO_6 octahedral tilting. Polyhedral zigzag chains are represented in light grey.

4.2. The complementary structure

As the two subgroups $P2_1cn$ and $P2_12_12_1$ are hemihedral, there is, for each of them, one complementary structure which corresponds to its image obtained through a symmetry element of the idealized group (*Pmcn*) which is not retained in the subgroup. Let us consider the crystals which were refined in the $P2_12_12_1$ enantiomorphic group (Fig. 10*a*).

How is it possible to imagine the simultaneous existence of both enantiomorphic components inside the same crystal? As these two components are images through an inversion element, one can choose any reflection plane or the symmetry centre. It is easy to see that through such an element the total octahedral tilting system may be reversed. The connection between the two structural components can be realized without difficulty at the level of a PO_4 tetrahedral slice (Fig. 10*b*), since it is naturally realized in the structure having the $P2_1cn$ group (Fig. 10*c*), as seen previously, keeping the 'pentagonal tunnels'. Another mode of connection has been proposed for γ-Mo_4O_{11} (Ghedira *et al.*, 1985). It is related to the existence of a stacking fault. If, in two adjacent slabs of WO_3-type, the set of octahedral segments remains parallel instead of adopting a chevron-type aspect (Fig. 10*d*), one obtains a connection which already exists in the MPTBh series, but with the introduction of a 'hexagonal tunnel', and the coexistence of the two enantiomorphic structural components. Whatever the joining process between the two enantiomorphic components may be, it is clear that the possible coexistence of these two forms within the crystal could be at the origin of some slight anomaly observed in the X-ray diffracted intensity for $P_4W_8O_{32}$ (m = 4) (Giroult *et al.*, 1981; de Boer, 1994). The previous development proposed for the two enantiomorphic components may be applied practically without change for $P_4W_4O_{20}$ (m = 2), whose total reverse structure is obtained through a (100) reflection plane or twofold axes parallel either to **b** or **c**. The connection between the two components may be realized, as previously, at the level of PO_4 tetrahedral slices.

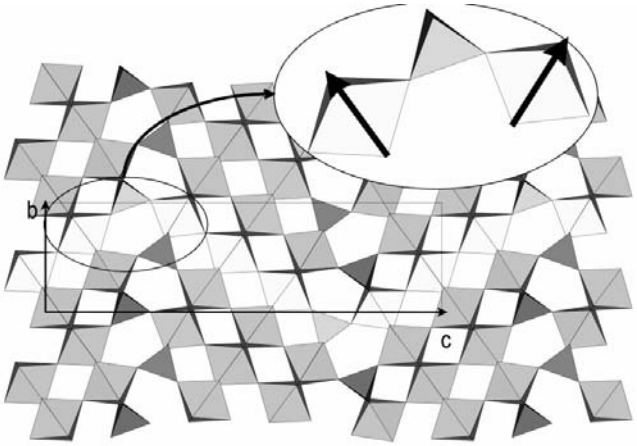

Figure 9
WO_6 octahedral tilting mode found in $P_4W_{12}O_{44}$ (m = 6, $P2_12_12_1$). Arrows are symbolic representations of the WO_6 octahedral tilting. Polyhedral zigzag chains are represented in light grey.

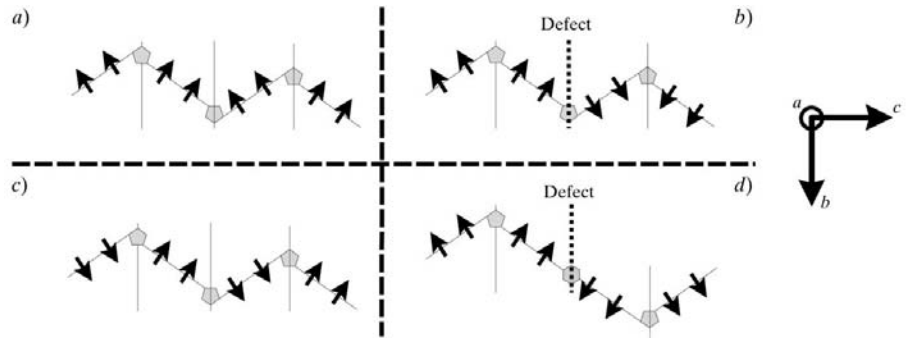

Figure 10
Different possible tilting modes in the successive slabs of the structure. Arrows are symbolic representations of the WO_6 octahedral tilting (see Figs. 8 and 9). (*a*) $P2_12_12_1$-type: the tilting direction remains the same from one slab to the next. (*b*) Local defect as the (001) mirror involving the change of tilting direction keeping the pentagonal tunnel shape. (*c*) $P2_1cn$-type: the tilting-sense is reversed from one slab to the next. (*d*) Local defect as found in MPTBh members leading to hexagonal-shaped tunnels.

5. The odd *m* members with *m* < 9

The odd m terms of the MPTBp series use exactly the same structural building principle as the even m terms. The major difference is that the WO_3-type slabs are no longer made of segments of the same length consisting of $m/2$ WO_6 octahedra as in the m even terms, but include segments of $(m + 1)/2$ and $(m - 1)/2$ octahedra (Fig. 5*b*). Within a slab, each $(m + 1)/2$ octahedral segment shares corners with four $(m - 1)/2$ octahedral segments and *vice versa*. This only atomic modification causes a total change in symmetry, a distortion of the orthorhombic lattice and generates the systematic existence of twins. If we again refer the actual structures to a hypothetical structural model where all the slabs are of the ReO_3-type, we find that the possible subgroups from the tilting mode of the octahedral segments are derived from the group $P2/m\ 2_1/n\ 2_1/n$ (Fig. 11*a*). As detailed elsewhere (Roussel *et al.*, 1996), the only octahedral rotation, also observed in all odd m members, destroys both the twofold axis parallel to **a** and the (100) mirror which is perpendicular without changing, however, the existence of the symmetry centre (Fig. 11*b*). Two centrosymmetric subgroups are then possible: $P2_1/n$ with **b** as the twofold axis and $P2_1/n$ with **c** as the twofold axis. These two subgroups have been effectively observed: the first one both for $P_4W_{10}O_{38}$ (m = 5; Roussel, Foury *et al.*, 1999) and for $P_4W_{14}O_{50}$ (m = 7; Roussel *et al.*, 1996); the second one for $(Mo,W)_9O_{25}$ (d'Yachenko *et al.*, 1995), which is an Mo structural counterpart of $P_4W_{14}O_{50}$ (m = 7), in which the tetrahedral site is Mo and the octahedral sites are mixed (Mo, W).

To compare the two polyhedral arrangement and, particularly, to scruti-

nize the difference between the octahedral tilting mode of the two structures, the comparison of $P_4W_{14}O_{50}$ (m = 7) and its Mo structural counterpart is instructive. A zigzag polyhedral chain along **c** is built up of three octahedra, one tetrahedron, four octahedra, one tetrahedron *etc.*, which are all located at the same x level (light grey in Figs. 12 and 13). As far as the tilt sense of the octahedra is concerned, one notices that within two successive slabs the rotation direction of the octahedral segments is symmetrical with respect to a (001) plane in $P_4W_{14}O_{50}$ (Fig. 12), whereas the inverse rotation is observed in $(Mo,W)_9O_{25}$ (Fig. 13). With respect to the tilting mode appearance, $P_4W_{14}O_{50}$ is directly comparable with the distribution observed in all the structures with even m which crystallize according to $P2_12_12_1$ (as in m = 4, 6 and 8), while for $(Mo,W)_9O_{25}$, the octahedral distribution is reminiscent of that found in m = 2 and γ-Mo_4O_{11} concerned with the group $P2_1cn$.

The simultaneous existence of different lengths for the octahedral segments inside the same slab and the tilting mode from one slab to the other induce a difference, with respect to the even m member, in the distribution of the PO_4 tetrahedra which are shifted in the (**a**, **b**) plane every second slice. This leads to a slight distortion of the orthorhombic lattice and to a monoclinic symmetry. However, the distortion remains weak, since the angular differences from 90° are 0.40, 0.19 and 0.18°, respectively, for $P_4W_{10}O_{38}$ (m = 5), $P_4W_{14}O_{50}$ (m = 7) and for $(Mo,W)_9O_{25}$ (m = 7). Note that for both MPTBp members the distortion takes place in the (**a**, **c**) plane, while for $(Mo,W)_9O_{25}$ it lies in the (**a**, **b**) plane.

5.1. Particular case of $P_4W_{10}O_{38}$ (m = 5)

All the previous considerations relative to the m = 5 member of the MPTBp family concern the pseudo-orthorhombic phase of this compound. Actually, another variety of this compound exists with exactly the same formula, $P_4W_{10}O_{38}$, but with a different crystal structure. This second variety is monoclinic with a β angle of 96.18° and corresponds to a structure composed of ordered successive slabs of WO_3-type arranged in a chevron-type manner as usual, but stacked as a regular intergrowth of m = 4 and m = 6 slabs (Benmoussa *et al.*, 1982). This variety has been called $2m = 4 + 6$ (Fig. 14*a*) as opposed to the pseudo-orthorhombic form named $2m = 5 + 5$ (Fig. 14*b*). This case is unique and has been only observed for $P_4W_{10}O_{38}$ (m = 5). However, some electron micrography patterns show that it can be obtained at

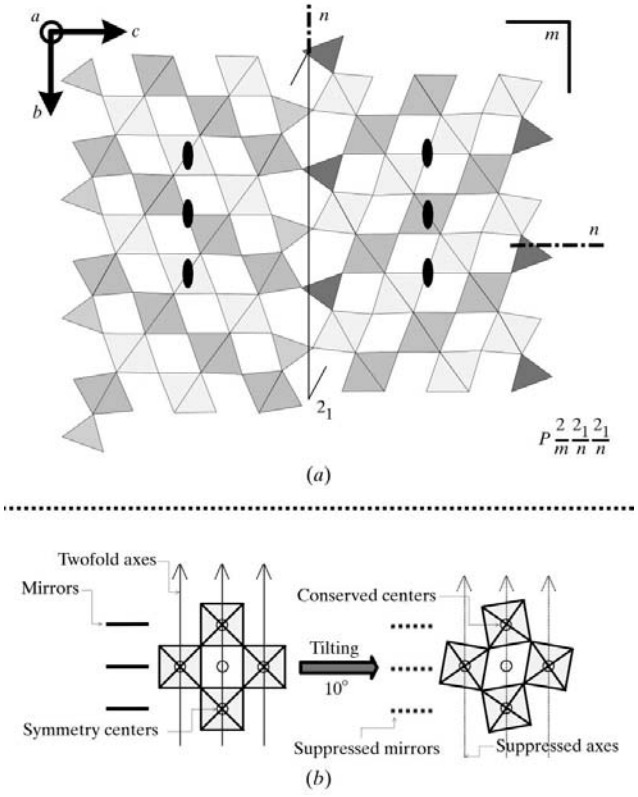

Figure 11
(*a*) Hypothetical structural model of an odd m member of the MPTBp series (here m = 7) and its related space group. (*b*) Schematic representation of the WO_6 octahedra in the idealized model (left) and in the actual tilted structure (right).

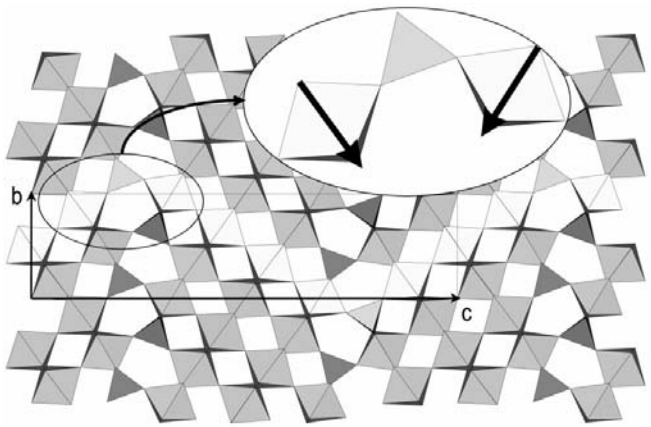

Figure 12
WO_6 octahedral tilting mode found in $P_4W_{14}O_{50}$ (m = 7) $P2_1/n$, $2_1 \parallel$ **b**. Arrows are symbolic representations of the WO_6 octahedral tilting. Polyhedral zigzag chains are represented in light grey.

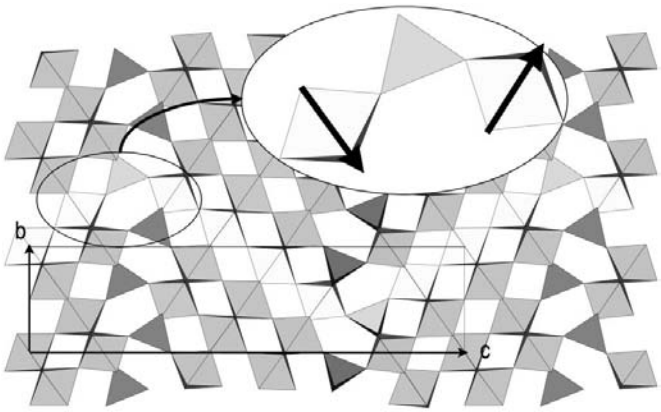

Figure 13
Tilting mode of the octahedra found in $(Mo,W)_9O_{25}$ $P2_1/n$, $2_1 \parallel$ **c**. Arrows are symbolic representations of the WO_6 octahedral tilting. Polyhedral zigzag chains are represented in light grey.

a local scale for other m values (Domengès *et al.*, 1984; Roussel *et al.*, 1998), suggesting that it may be *a priori* possible to obtain each member of the MPTBp family whatever the m value with two distinct layer forms, one being more stable than the other.

5.2. The twins

In the diffraction patterns of the investigated MPTBp odd m members, there always appears a splitting of some reflections. This phenomenon has been interpreted as a twinning effect, which is related to the pseudo-orthorhombic character of the structure. Indeed, the distribution of the spots in the reciprocal lattice has been the subject of meticulous investigations using a CAD-4 X-ray diffractometer. The observations are consistent with a twin law where the **a** and **b** parameters of the two monoclinic components of the twin are merged whereas the two **c** parameters are separated and make an angle of 0.80° in $P_4W_{10}O_{38}$ (m = 5) and 0.38° in $P_4W_{14}O_{50}$ (m = 7).

The structural relations between the two components of the twin are still related to the tilting mode of octahedral segments. Starting with the model in Fig. 12 (m = 7), taken as an example, which is consistent with the group $P2_1/n$ (with the twofold axis along **b**), it is easy to see that the image of this model through a (100) or (001) mirror or through a binary rotation along **a** or **c** leads to a model in which all the polyhedra are tilted in the other direction. However, there are two major differences with the twin cases already encountered for the even m members of the series. Firstly, this new model also has the symmetry $P2_1/n$ and is exactly identical to the one in Fig. 12. Both models are indeed related through a 180° rotation about **a** or through a symmetry with respect to the (**a**, **b**) plane. In the even m members the two models of the twin are complementary but not identical. Secondly, the two twinned lattices being monoclinic and no longer orthorhombic, they are not exactly superimposed as for the even m members: a splitting effect of the reflections in the diffraction patterns is observed, except in the (100)* twin plane. As mentioned above, the phosphate slice is an ideal plane in the structure to initiate the reverse of the octahedral segments tilting and the phenomenon may be produced several times during the crystal growth process in a repeated way from different (001) PO_4 planes, generating a polysynthetic twin.

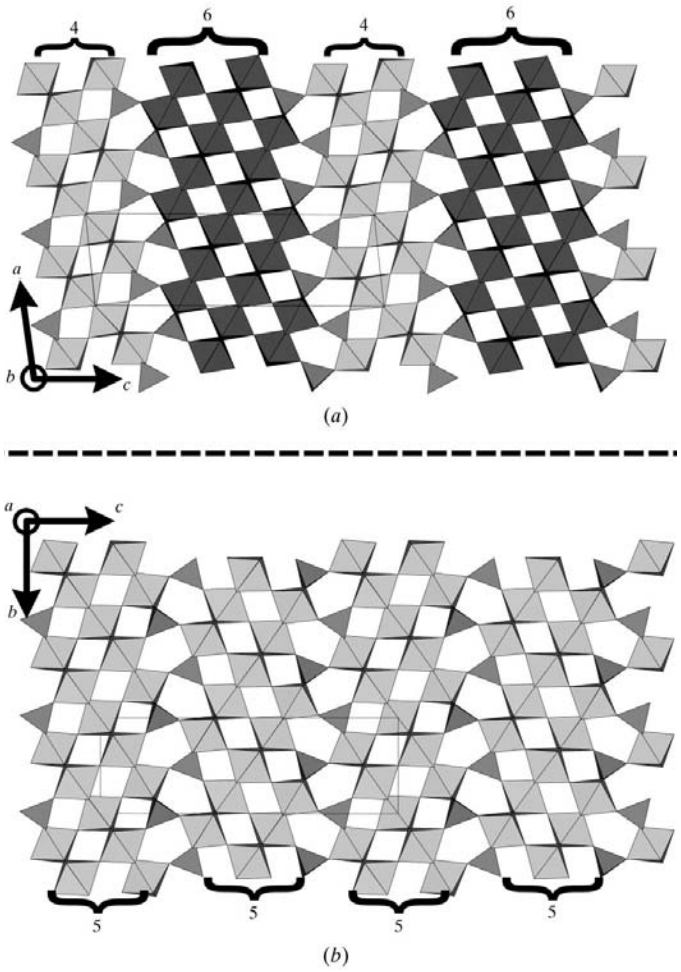

Figure 14
Projections of the two varieties of $P_4W_{10}O_{38}$: (*a*) $2m$ = 4 + 6; (*b*) $2m$ = 5 + 5.

The numerous investigated crystals of the $(PO_2)_4(WO_3)_{2m}$ series with odd m, in order to choose the best sample before starting a detailed structural study, show that all the samples were twinned. This phenomenon has led to the assertion that the lattices of all these odd m members of the series with $m < 9$ were effectively monoclinic pseudo-orthorhombic with a related symmetry, the twofold axis always being along **b** and to a better understanding of the previous features, and in particular an interpretation of the structural properties generating the twin process. However, it also creates a difficulty in the intensity measurement and in the resolution process, since one must take into account the existence of the two components of the twin. Moreover, it is worth noting that the crystals of $(Mo,W)_9O_{25}$ [the (Mo,W) counterpart of the m = 7 member] which support the monoclinic $P2_1/n$ group now with 2_1 along **c** (d'Yachenko *et al.*, 1995) are not reported as being twinned. This fact seems, *a priori*, strange since, as for $P_4W_{14}O_{50}$, one can imagine a model deduced from that in Fig. 13 through a binary rotation about **a**, involving the reverse tilt of all the octahedral segments, and it seems logical to obtain the same twin phenomenon in joining these two structural blocks either for $P_4W_{10}O_{38}$ (m = 5) or $P_4W_{14}O_{50}$ (m = 7). However, an important difference exists between these two cases. In the MPTBp series the monoclinic (**a**, **b**) plane of the lattice includes a γ angle between **a** and **b** with a value of exactly 90°, and the joining of the two structural blocks can be realized along a PO_4 slice without distortion at all, the two monoclinic lattices lying symmetrically with respect to the PO_4 slice. However, for $(Mo,W)_9O_{25}$, the monoclinic (**a**, **b**) plane includes a γ angle with a value different from 90° (90.18°), involving too strong a local strain at the level of the PO_4 slice where the two lattices are joined, since two axes, *e.g.* **b** and **b**′, should form an angle of 0.36°.

This interpretation seems to be confirmed by the following study of the m = 9 member of the series $P_4W_{18}O_{62}$.

6. X-ray structural determination of $P_4W_{18}O_{62}$ (m = 9)

The structural knowledge of the m = 9 compound of the MPTBp series was desirable because the compounds with m > 9 were affected by a pseudo-orthorhombic symmetry with a γ monoclinic distortion (Table 1) whereas, as mentioned above, the terms with m < 9 were either strictly orthorhombic or monoclinic with a β distortion. In this context it seemed important to find out both the true symmetry and the structural configuration of the WO_6 octahedral segments in the m = 9 compound. A crystal with the composition $P_4W_{18}O_{62}$ was studied by conventional single-crystal X-ray techniques, using both film patterns from a Weissenberg method and a CAD-4 diffractometer. As previously observed for $P_4W_{24}O_{80}$, the m = 12 member of the series, the selected crystal corresponds to the high-temperature form, *i.e.* without satellite reflections (Roussel *et al.*, 1998).

6.1. Lattice and twin study

The photographs, taken using a Weissenberg camera, with the crystal rotating most often about **a** + **b**, were complex and not easy to interpret. The observed splitting of the spots suggested a twin, but the twin law was difficult to find and clearly less evident than those observed in m = 5 or m = 7. The use of the diffractometric data, testing the $P2_1/n$ group with the twofold axis either along **b** or along **c** and taking the twin effects into account, gave unsatisfactory results. Moreover, the parameters of the monoclinic cell did not refine properly. The problem was solved, for the most part, when it was assumed that the crystal could be triclinic with an α angle of 90°, a β angle (90.20°) very close to that observed in m = 7 and a γ angle clearly different from 90° (90.25° or 89.75° according to the reference axes). The twin law was exactly the same as that of m = 5 and m = 7, *i.e.* corresponds to a monoclinic distortion with a β angle different from 90° and with the (001) plane as the twin element.

6.2. Results and discussion

A summary of the data and appropriate parameters for the structure determination are given in Table 2.[1] The group retained for the structure refinement was finally $P\bar{1}$ which is also a subgroup of $P2_1/n$. The application of the twin matrix using the program *JANA98* (Petricek & Dusek, 1999), taking into account the two sets of Bragg reflections, collected together, settles down a twin ratio of 0.25 which seems suitable according to the films observations.

The results of the last refinement are given in Tables 3 and 4. Note that the O atoms O2*a* and O3*a* and also their pseudo-equivalents O2*b* and O3*b* cannot be refined and moved to diverging coordinates. Their positions have been fixed according to those deduced from the difference Fourier series. As seen in Fig. 15, these O atoms are all apices of the PO_4 tetrahedra.

[1] Supplementary data for this paper are available from the IUCr electronic archives (Reference: LC0016). Services for accessing these data are described at the back of the journal.

Table 2
Experimental details.

Crystal data	
Chemical formula	$P_4W_{18}O_{62}$
Chemical formula weight	4425.1
Cell setting	Triclinic
Space group	$P\bar{1}$
a (Å)	5.2945 (9)
b (Å)	6.542 (2)
c (Å)	32.744 (5)
α (°)	90.00 (2)
β (°)	90.20 (2)
γ (°)	89.78 (2)
V (Å^3)	1134.2 (4)
Z	1
D_x (Mg m^{-3})	6.477
Radiation type	Mo $K\alpha$
Wavelength (Å)	0.71073
μ (mm^{-1})	45.714
Temperature (K)	293
Crystal form	Platelet
Crystal size (mm)	0.158 × 0.144 × 0.004
Crystal colour	Dark blue
Data collection	
Diffractometer	Enraf–Nonius CAD-4
Absorption correction	Gaussian
T_{min}	0.148
T_{max}	0.833
No. of measured reflections	20 410
No. of independent reflections	20 041
No. of observed reflections	4661
Criterion for observed reflections	$I > 3\sigma(I)$
θ_{max} (°)	45
Range of h, k, l	$0 \rightarrow h \rightarrow 10$ $-12 \rightarrow k \rightarrow 12$ $-64 \rightarrow l \rightarrow 64$
Reflection for crystal matrix orientation ($5 < 2\theta < 43°$)	17
No. of standard reflections	3
Frequency of standard reflections	Every 60 min
Refinement	
Refinement on	F
R	0.0572
wR	0.0468
S	2.79
No. of reflections used in refinement	4661
No. of parameters used	200
Weighting scheme	$w = 1/\sigma^2(F_o)$
$(\Delta/\sigma)_{max}$	0.001
$\Delta\rho_{max}$ (e Å^{-3})	1.443
$\Delta\rho_{min}$ (e Å^{-3})	−1.340
Twin matrix	$(001)(010)(00\bar{1})$
Twin ratio	0.25 (1)
Source of atomic scattering factors	*International Tables for Crystallography* (1992, Vol. C)
Computer programs	
Data collection	*CAD*-4 (Enraf–Nonius, 1989)
Cell refinement	*SET*4 (Enraf–Nonius, 1989)

The structure of $P_4W_{18}O_{62}$ is in good agreement with those of all the members of the MPTBp family, and in particular with that of the m = 5 and m = 7 members. However, with respect to the polyhedral arrangement of these two last compounds, it should be pointed out that two successive slabs of WO_3-type are now symmetrically independent and no longer related to a 2_1 axis or a glide plane. There remains only a symmetry centre in the middle of the slab either on a W position or on an O

Table 3
Fractional atomic coordinates and equivalent isotropic displacement parameters (Å^2).

	x	y	z	U_{eq}
W1*a*	0.0038 (2)	0.3258 (2)	0.81485 (3)	0.0084 (3)†
W2*a*	0.4992 (2)	−0.0139 (2)	0.86117 (4)	0.0092 (3)†
W3*a*	0.0040 (2)	−0.3425 (2)	0.90852 (4)	0.0107 (3)†
W4*a*	0.4996 (2)	−0.3287 (2)	0.04583 (4)	0.0110 (4)†
W5*a*	0	0	0	0.0120 (5)†
W1*b*	0.5061 (2)	0.8257 (1)	0.68501 (4)	0.0071 (3)†
W2*b*	0.0083 (2)	0.4876 (2)	0.63874 (4)	0.0097 (3)†
W3*b*	0.5021 (2)	0.1572 (2)	0.59152 (4)	0.0104 (3)†
W4*b*	0.0023 (2)	0.8289 (2)	0.54569 (4)	0.0115 (4)†
W5*b*	1/2	1/2	1/2	0.0115 (4)†
P*a*	0.499 (1)	−0.3636 (8)	0.7832 (2)	0.0008 (9)
P*b*	0.011 (1)	0.1369 (9)	0.7173 (2)	0.004 (1)
O1*a*	0.239 (3)	0.531 (2)	0.7873 (5)	0.018 (4)
O2*a*‡	0.732	−0.489	0.7927	0.013
O3*a*‡	−0.013	0.208	0.7596	0.013
O4*a*	0.998 (4)	−0.497 (3)	0.8578 (7)	0.021 (5)
O5*a*	0.783 (3)	0.142 (2)	0.8367 (5)	0.008 (3)
O6*a*	0.276 (4)	0.175 (3)	0.8321 (6)	0.023 (4)
O7*a*	0.511 (4)	−0.169 (3)	0.8088 (7)	0.019 (5)
O8*a*	0.501 (3)	0.163 (2)	0.9041 (6)	0.008 (4)
O9*a*	0.721 (3)	−0.192 (2)	0.8836 (5)	0.008 (3)
O10*a*	0.214 (3)	−0.147 (2)	0.8797 (5)	0.016 (3)
O11*a*	0.998 (3)	−0.166 (3)	0.9519 (6)	0.010 (4)
O12*a*	0.789 (3)	−0.533 (2)	0.9330 (4)	0.007 (2)
O13*a*	0.287 (3)	−0.474 (2)	0.9253 (4)	0.008 (3)
O14*a*	1/2	−1/2	0	0.021 (7)
O15*a*	0.215 (3)	0.192 (2)	0.9734 (5)	0.008 (3)
O16*a*	0.287 (3)	−0.137 (2)	0.0197 (5)	0.007 (3)
O1*b*	0.275 (3)	0.028 (2)	0.7126 (5)	0.015 (3)
O2*b*‡	0.809	0.982	0.7074	0.013
O3*b*‡	0.498	0.69	0.7386	0.013
O4*b*	0.518 (3)	0.991 (2)	0.6403 (6)	0.010 (4)
O5*b*	0.233 (3)	0.679 (2)	0.6714 (4)	0.007 (3)
O6*b*	0.733 (3)	0.641 (2)	0.6650 (5)	0.010 (3)
O7*b*	0.995 (4)	0.323 (3)	0.6897 (7)	0.018 (5)
O8*b*	0.005 (3)	0.662 (3)	0.5957 (7)	0.011 (5)
O9*b*	0.790 (3)	0.305 (2)	0.6159 (5)	0.013 (3)
O10*b*	0.291 (3)	0.351 (2)	0.6236 (4)	0.006 (2)
O11*b*	0.506 (3)	0.329 (3)	0.5470 (6)	0.011 (5)
O12*b*	0.718 (2)	0.973 (2)	0.5682 (4)	0.005 (3)
O13*b*	0.214 (2)	0.022 (2)	0.5749 (4)	0.003 (2)
O14*b*	0	0	0.5	0.014 (6)
O15*b*	0.787 (3)	0.637 (2)	0.5219 (5)	0.013 (3)
O16*b*	0.286 (3)	0.688 (2)	0.5288 (4)	0.006 (3)

	U^{11}	U^{22}	U^{33}	U^{12}	U^{13}	U^{23}
W1*a*	0.0110 (5)	0.0092 (5)	0.0051 (5)	0.0033 (4)	−0.0002 (4)	−0.0019 (4)
W2*a*	0.0141 (5)	0.0068 (4)	0.0066 (4)	0.0016 (4)	−0.0017 (4)	−0.0025 (4)
W3*a*	0.0128 (6)	0.0100 (5)	0.0093 (6)	0.0042 (5)	−0.0037 (5)	−0.0040 (4)
W4*a*	0.0135 (7)	0.0106 (5)	0.0088 (7)	0.0030 (5)	−0.0028 (5)	−0.0046 (5)
W5*a*	0.0126 (8)	0.0130 (7)	0.0103 (8)	0.0040 (6)	−0.0028 (7)	−0.0055 (7)
W1*b*	0.0079 (5)	0.0067 (4)	0.0067 (5)	0.0004 (4)	0.0029 (4)	0.0004 (4)
W2*b*	0.0111 (5)	0.0082 (5)	0.0096 (5)	0.0035 (4)	0.0037 (4)	0.0044 (4)
W3*b*	0.0144 (6)	0.0093 (5)	0.0074 (6)	0.0030 (5)	0.0041 (5)	0.0030 (4)
W4*b*	0.0137 (7)	0.0124 (6)	0.0084 (7)	0.0064 (5)	0.0048 (5)	0.0053 (4)
W5*b*	0.0165 (9)	0.0135 (8)	0.0045 (7)	0.0079 (7)	0.0040 (6)	0.0058 (6)

† $U_{eq} = (1/3)\Sigma_i\Sigma_j U^{ij} a^i a^j \mathbf{a}_i.\mathbf{a}_j$. ‡ Positions deduced from the Fourier-difference series.

position. It was then necessary to solve the problem of the actual configuration of the tilt mode in the successive octahedral segments and to determine if it corresponds to a $P_4W_{14}O_{50}$-type or rather to a $(Mo,W)_9O_{25}$-type. The solution was found from Fourier-difference series, by testing systematically the area around each O atom after the position refinement of all the W atoms. As shown in Fig. 16, for one of the O atoms, the octahedral configuration of the m = 7 compound gives a unique peak (Fig. 16*a*), whereas two split positions (Fig. 16*b*) are obtained for the $(Mo,W)_9O_{25}$-type. The right configuration of the polyhedra is illustrated in Fig. 15.

At first sight, compared with $(Mo,W)_9O_{25}$, it seems paradoxical that a twin effect can be realized in $P_4W_{18}O_{62}$. Indeed, as shown previously for $(Mo,W)_9O_{25}$, the angular difference from 90° of the γ angle creates in the composition plane (confused with one tetrahedral PO_4 slice) an unrealizable local strain. However, in spite of the γ angle, the configuration of the WO_6 octahedral segments in $P_4W_{18}O_{62}$ is clearly different from that involved in $(Mo,W)_9O_{25}$. It is rather similar to the one of the odd m members of the series. Thus, if a model of the m = 9 compound is supposed in which all the segments consist of the reverse tilting of all the WO_6 octahedra, then the two models are the images of one another through a (001) mirror, *i.e.* a PO_4 slice plane which can be chosen as a composition common plane (Fig. 17). The two rows **a** and **b** are not at right angles, but it does not matter because they are included in the twin plane, whereas in $(Mo,W)_9O_{25}$ this same plane could not be the twin plane because it was already a mirror plane in its symmetry group.

7. The members with $m > 9$

For $m > 9$, the structures which have been solved correspond to m = 10 ($P_4W_{20}O_{68}$; Roussel *et al.*, 2000) and m = 12 ($P_4W_{24}O_{80}$; Roussel *et al.*, 1998). X-ray data have been collected for m = 13, and also for m = 14, but without confirmation of the atomic arrangement at the present time (Roussel, Labbé & Groult, 1999). However, if for m = 12 ($P_4W_{24}O_{80}$) the structure has been refined in the orthorhombic symmetry $P2_12_12_1$, like that described for other even m members (m = 4, 6, 8), the members m = 10, 13, 14 show complex diffraction patterns with satellite reflections, involving modulated struc-

tures (Table 1). In this context the m = 12 member could also display a modulated structure at room temperature since the two transition temperatures observed from X-ray diffuse scattering experiments are 500 and 535 K.

The modulated phase of $P_4W_{20}O_{68}$ involves a γ distortion of the orthorhombic lattice, like for the modulated forms of m = 12, 13 and 14. This feature induces that the same phenomenon can arise for all these $m > 9$ compounds. The characteristic underlined from a four-dimensional treatment in the m = 10 compound is that the modulation acts only on the displacement of the W atoms, taking place in a segment of ten WO_6 octahedra within a slab of WO_3-type. Such segments may be gathered in planes parallel either to (110) or to ($\bar{1}$10). In the ideal structure these planes are symmetrically equivalent, but from the W displacements this property disappears and the monoclinic distortion with a γ angle different from 90° becomes possible. Moreover, the anionic sublattice is apparently not disturbed by the modulation and consequently the tilting mode found for this compound is exactly the same as the one corresponding to all the m even members of the series, in spite of a different space group of the average structure ($P2_1$ rather than $P2_12_12_1$).

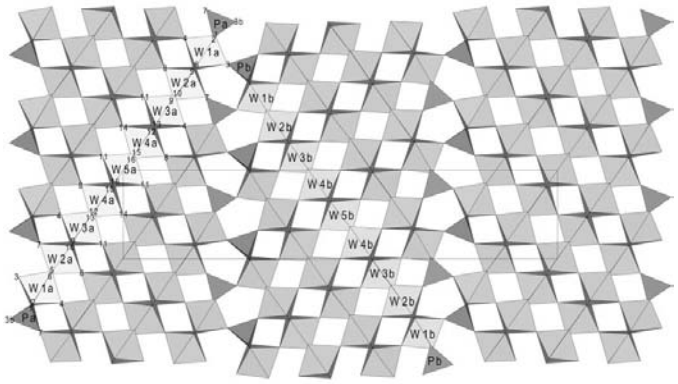

Figure 15
Projection onto (100) of $P_4W_{18}O_{62}$ (m = 9).

As for $P_4W_{18}O_{62}$ (m = 9), the twin phenomenon may arise, starting from a PO_4 slice; this slice is as a privileged plane to initiate the inversion of the tilting mode from one WO_3-type slab to another. Thus, one can build, by reflection through a (001) mirror, the twinned model (which is non-superimposable since enantiomorphic) where all the WO_6 octahedra are rotated in the reverse direction. The twinned crystal is then realized by joining the two components at the level of a PO_4 slice. As previously seen, the value of the γ angle does not matter because the distortion takes place inside the twin plane and consequently without constraint. The numerous crystals tested at room temperature for high-m members confirm that the twin arises in all the samples, and although it is rather difficult to clearly observe its effects, particularly in the Weissenberg photographs.

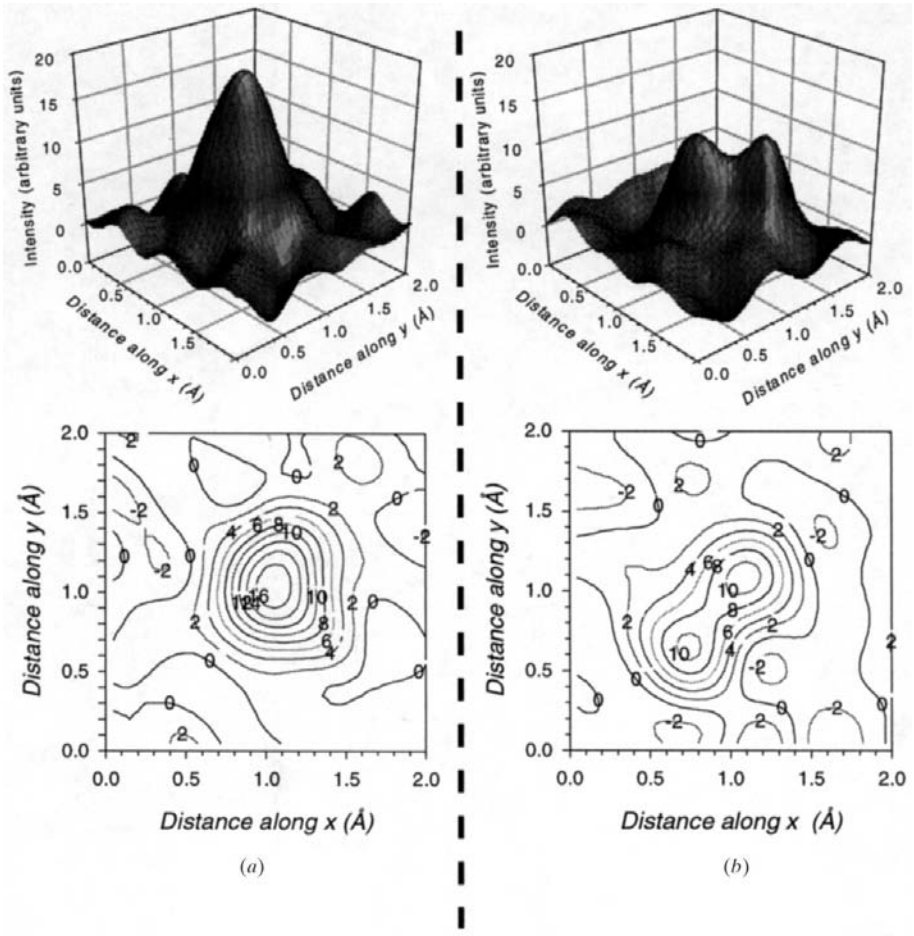

Figure 16
Fourier difference map around O16a. (a) $P_4W_{14}O_{50}$ configuration; (b) $(Mo,W)_9O_{25}$ configuration.

8. Conclusions

The present work is devoted to a survey of the different crystal symmetries encountered in the members of the MPTBp family $(PO_2)_4(WO_3)_{2m}$ with $2 \leq m \leq 14$.

For the high-temperature forms, corresponding to $T > T_c$, where T_c is the critical transition temperature found from X-ray diffuse scattering, an important difference is underlined between the even and the odd m members. Although the building principle is exactly the same, the even members are shown to crystallize with $P2_1cn$ or $P2_12_12_1$ groups, *i.e.* non-centrosymmetrical orthorhombic groups, while odd m members have the centrosymmetrical monoclinic group $P2_1/n$. In this latter case the result is a distortion of the orthorhombic lattice either in the (**a**, **c**) plane or in the (**a**, **b**) plane leading to an interpretation in

Table 4
Selected interatomic distances (Å) and standard uncertainties for $P_4W_{18}O_{62}$.

W1*a*—O1*a*	2.05 (1)	W1*b*—O1*b*	2.02 (1)
W1*a*—O2*a*	2.01 (2)	W1*b*—O2*b*	2.04 (2)
W1*a*—O3*a*	1.97 (3)	W1*b*—O3*b*	1.97 (1)
W1*a*—O4*a*	1.82 (2)	W1*b*—O4*b*	1.82 (2)
W1*a*—O5*a*	1.83 (1)	W1*b*—O5*b*	1.79 (1)
W1*a*—O6*a*	1.83 (2)	W1*b*—O6*b*	1.82 (1)
W2*a*—O5*a*	1.99 (2)	W2*b*—O5*b*	2.03 (1)
W2*a*—O6*a*	1.95 (2)	W2*b*—O6*b*	1.97 (2)
W2*a*—O7*a*	1.99 (2)	W2*b*—O7*b*	1.99 (2)
W2*a*—O8*a*	1.82 (2)	W2*b*—O8*b*	1.81 (2)
W2*a*—O9*a*	1.81 (1)	W2*b*—O9*b*	1.82 (1)
W2*a*—O10*a*	1.85 (2)	W2*b*—O10*b*	1.81 (2)
W3*a*—O4*a*	1.94 (2)	W3*b*—O4*b*	1.93 (2)
W3*a*—O9*a*	1.96 (2)	W3*b*—O9*b*	1.97 (2)
W3*a*—O10*a*	1.94 (1)	W3*b*—O10*b*	1.99 (1)
W3*a*—O11*a*	1.83 (2)	W3*b*—O11*b*	1.84 (2)
W3*a*—O12*a*	1.87 (1)	W3*b*—O12*b*	1.83 (1)
W3*a*—O13*a*	1.81 (2)	W3*b*—O13*b*	1.85 (1)
W4*a*—O8*a*	1.97 (2)	W4*b*—O8*b*	1.97 (2)
W4*a*—O12*a*	1.91 (1)	W4*b*—O12*b*	1.92 (1)
W4*a*—O13*a*	1.95 (1)	W4*b*—O13*b*	1.94 (1)
W4*a*—O14*a*	1.873 (1)	W4*b*—O14*b*	1.868 (1)
W4*a*—O15*a*	1.87 (2)	W4*b*—O15*b*	1.87 (1)
W4*a*—O16*a*	1.89 (1)	W4*b*—O16*b*	1.85 (1)
W5*a*—O11*a* (×2)	1.91 (2)	W5*b*—O11*b* (×2)	1.90 (2)
W5*a*—O15*a* (×2)	1.91 (1)	W5*b*—O15*b* (×2)	1.91 (2)
W5*a*—O16*a* (×2)	1.87 (2)	W5*b*—O16*b* (×2)	1.92 (1)
P*a*—O1*a*	1.55 (2)	P*b*—O1*b*	1.57 (2)
P*a*—O2*a*	1.51 (2)	P*b*—O2*b*	1.51 (2)
P*a*—O7*a*	1.53 (2)	P*b*—O7*b*	1.52 (2)
P*a*—O3*b*	1.50 (1)	P*b*—O3*a*	1.47 (3)

terms of tilting of the WO_6 octahedral segments. A structural model is proposed to explain the existence of twins for the most part of these compounds. For the even *m* structures the two lattice components are exactly superimposed and the discrimination resulting in an absolute structure is bound to the anomalous dispersion factors. For the odd *m* members the two monoclinic lattices are separated, and result in a splitting effect in the diffraction patterns. Elsewhere, the absence of twins in $(Mo,W)_9O_{25}$ is also justified.

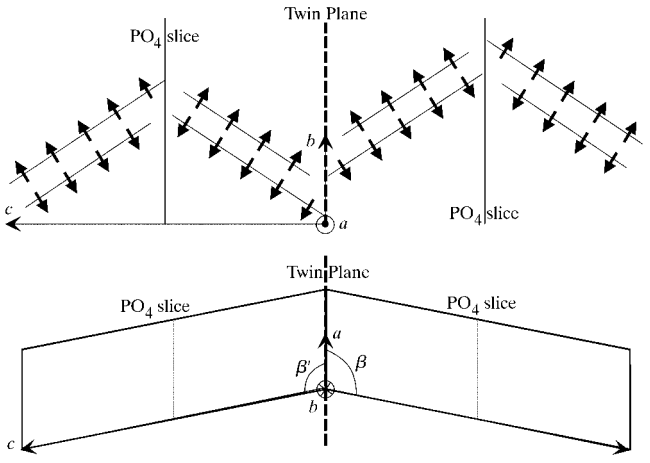

Figure 17
Twin model proposed for $P_4W_{18}O_{62}$ (m = 9).

The existence at room temperature of two forms for $P_4W_{10}O_{38}$, one with slabs of regular thickness ($2m = 5 + 5$) and the other one with slabs of different thickness ($2m = 4 + 6$), suggests strongly that the different *m* members could crystallize with several forms, one being pseudo-orthorhombic and the other being clearly monoclinic. However, the fact that one obtains most often the form with equal slab thickness implies that this regular form is probably the most stable.

For the low-temperature forms, below T_c, it seems, on the basis of the m = 10 study, that all the *m* members of the series are likely to be endowed with a modulated structure. The origin of this instability takes place in the ordered displacement of all the W atoms within the WO_6 octahedra and particularly in a segment of *m* octahedra bounded at each end by a PO_4 tetrahedron, creating a ferroelectric average polarization. The correlated distortion is monoclinic with a γ angle different from 90°.

To confirm these assertions it should be useful to know precisely other structures, particularly m = 11, 12 (monoclinic form), 13 and 14, but also the low-temperature forms of weak *m* values. All these phases should present satellite reflections in the diffraction patterns involving modulation phenomena, probably strongly related to ferroelectric antiferroelectric instabilities.

References

Beierlein, U., Schlenker, C., Dumas, J., Groult, D., Labbé, Ph., Balthes, E. & Steep, E. (1999). *Synth. Met.* **103**, 2593–2595.
Benmoussa, A., Labbé, Ph., Groult, D. & Raveau, B. (1982). *J. Solid State Chem.* **44**, 318–325.
Boer, J. de (1994). Private communication.
Diehl, R., Brandt, G. & Salje, E. (1978). *Acta Cryst.* B**34**, 1105–1111.
Domengès, B., Goreaud, M., Labbé, Ph. & Raveau, B. (1982). *Acta Cryst.* B**38**, 1724–1728.
Domengès, B., Hervieu, M., Raveau, B. & O'Keeffe, M. (1988). *J. Solid State Chem.* **72**, 155–172.
Domengès, B., Hervieu, M., Raveau, B. & Tilley, R. J. D. (1984). *J. Solid State Chem.* **54**, 10–28.
Domengès, B., Roussel, P., Labbé, Ph. & Groult, D. (1996). *J. Solid State Chem.* **127**, 302–307.
Enraf–Nonius (1989). *CAD-4 Software*. Version 5.0. Enraf–Nonius, Delft, The Netherlands.
Favre-Nicolin, V. & Hodeau, J. L. (1998). Private communication.
Foury, P. (1993). PhD thesis. Paris-V University, France.
Foury, P. & Pouget, J. P. (1993). *Int. J. Mod. Phys. B*, **7**, 3973–4003.
Foury, P., Pouget, J. P., Teweldemedhin, Z. S., Wang, E. & Greenblatt, M. (1993). *Synth. Met.* **55/57**, 2605–2610.
Foury, P., Pouget, J. P., Teweldemedhin, Z. S., Wang, E., Greenblatt, M. & Groult, D. (1993). *J. Phys. IV*, **3**, 133–136.
Foury, P., Pouget, J. P., Wang, E. & Greenblatt, M. (1991). *Synth. Met.* **41/43**, 3973–3974.
Foury, P., Pouget, J. P., Wang, E. & Greenblatt, M. (1992). *Europhys. Lett.* **16**, 485–490.
Foury, P., Roussel, P., Groult, D. & Pouget, J. P. (1999). *Synth. Met.* **103**, 2624–2627.
Ghedira, M., Vincent, H., Marezio, M., Marcus, J. & Furcaudot, G. (1985). *J. Solid State Chem.* **56**, 66–73.
Giroult, J. P., Goreaud, M., Labbé, Ph. & Raveau, B. (1981). *Acta Cryst.* B**37**, 2139–2142.
Glazer, A. M. (1972). *Acta Cryst.* B**28**, 3384–3392.

Greenblatt, M. (1993). Editor. *Oxide Bronzes.* Singapore: World Scientific.
Hess, C. (1997). PhD thesis. Grenoble University, France.
Hess, C., Le Touze, C., Schlenker, C., Dumas, J. & Groult, D. (1997). *Synth. Met.* **86**, 2157–2158.
Hess, C., Le Touze, C., Schlenker, C., Dumas, J., Groult, D. & Marcus, J. (1997). *Synth. Met.* **86**, 2419–2422.
Hess, C., Schlenker, C., Bonfait, G., Marcus, J., Ohm, T., Paulsen, C., Dumas, J., Tholence, J. L., Greenblatt, M. & Almeida, M. (1997). *Physica C*, **282/287**, 955–956.
Hess, C., Schlenker, C., Bonfait, G., Ohm, T., Paulsen, C., Dumas, J., Teweldemedhin, Z. S., Greenblatt, M., Marcus, J. & Almeida, M. (1997). *Solid State Commun.* **104**, 663–668.
Hess, C., Schlenker, C., Dumas, J., Greenblatt, M. & Teweldemedhin, Z. S. (1996). *Phys. Rev. B*, **54**, 4581–4588.
Hess, C., Schlenker, C., Hodeau, J. L., Ottolenghi, A. & Pouget, J. P. (1997). *Synth. Met.* **86**, 2169–2170.
Kehl, W. L., Hay, R. G. & Wahl, D. (1952). *J. Appl. Phys.* **23**, 212–215.
Kinomura, N., Hirose, M., Kumada, N., Muto, F. & Ashida, T. (1988). *J. Solid State Chem.* **77**, 156–161.
Labbé, Ph., Goreaud, M. & Raveau, B. (1986). *J. Solid State Chem.* **61**, 324–331.
Lehmann, J., Schlenker, C., Le Touze, C., Rötger, A., Dumas, J., Marcus, J., Teweldemedhin, Z. S. & Greenblatt, M. (1993). *J. Phys. IV*, **3**, 243–246.
Le Touze, C. (1996). PhD thesis. Grenoble University, France.
Le Touze, C., Bonfait, G., Schlenker, C., Dumas, J., Almeida, M., Greenblatt, M. & Teweldemedhin, Z. S. (1995). *J. Phys. IV*, **5**, 437–442.
Loopstra, B. O. & Rietveld, H. M. (1969). *Acta Cryst.* B**25**, 1420–1421.
Ludecke, J., Jobst, A. & van Smaalen, S. (2000). *Eur. Phys. Lett.* **49**, 357–361.
Magnéli, A. (1949). *Arkiv Kemi.* pp. 213–221.
Ottolenghi, A. (1996). PhD thesis. Paris-V University, France.
Ottolenghi, A., Foury, P., Pouget, J. P., Teweldemedhin, Z. S., Greenblatt, M., Groult, D., Marcus, J. & Schlenker, C. (1995). *Synth. Met.* **70**, 1301–1302.
Ottolenghi, A. & Pouget, J. P. (1996). *J. Phys. IV*, **6**, 1059–1083.
Petricek, V. & Dusek, M. (1999). *JANA98.* Institute of Physics, Praha, Czech Republic.
Rötger, A., Lehmann, J., Schlenker, C., Dumas, J., Marcus, J., Teweldemedhin, Z. S. & Greenblatt, M. (1994). *Europhys. Lett.* **25**, 23–29.
Rötger, A., Schlenker, C., Dumas, J., Wang, E., Teweldemedhin, Z. S. & Greenblatt, M. (1993). *Synth. Met.* **55/57**, 2670–2675.
Roussel, P., Foury, P., Groult, D., Pouget, J. P. & Labbé, Ph. (1999). *Eur. Phys. J. B*, **12**, 497–509.
Roussel, P., Groult, D., Maignan, A. & Labbé, Ph. (1999). *Chem. Mater.* **11**, 2049–2056.
Roussel, P., Labbé, Ph. & Groult, D. (1999). Unpublished results.
Roussel, P., Labbé, Ph., Groult, D., Domengès, B., Leligny, H. & Grebille, D. (1996). *J. Solid State Chem.* **122**, 281–290.
Roussel, P., Labbé, Ph., Leligny, H., Groult, D., Foury, P. & Pouget, J. P. (2000). *Phys. Rev. B.* In the press
Roussel, P., Mather, G., Domengès, B., Groult, D. & Labbé, Ph. (1998). *Acta Cryst.* B**54**, 365–375.
Salje, E. (1977). *Acta Cryst.* B**33**, 574–577.
Schlenker, C. (1989). Editor. *Low-Dimensional Electronic Properties of Molybdenum Bronzes and Oxides*, Vol. 11. Dordrecht: Kluwer.
Schlenker, C., Dumas, J., Greenblatt, M. & van Smaalen, S. (1996). *Physics and Chemistry of Low Dimensional Inorganic Conductors*, NATO ASI Series. New York: Plenum Press.
Schlenker, C., Hess, C., Le Touze, C. & Dumas, J. (1996). *J. Phys. IV*, **6**, 2061–2078.
Schlenker, C., Le Touze, C., Hess, C., Rötger, A., Dumas, J., Marcus, J., Greenblatt, M., Teweldemedhin, Z. S., Ottolenghi, A., Foury, P. & Pouget, J. P. (1995). *Synth. Met.* **70**, 1263–1266.
Teweldemedhin, Z. S., Ramanujachary, K. V. & Greenblatt, M. (1991). *J. Solid State Chem.* **95**, 21–28.
Teweldemedhin, Z. S., Ramanujachary, K. V. & Greenblatt, M. (1992). *Phys. Rev. B*, **46**, 7897–7900.
Vogt, T., Woodward, M. & Hunter, B. A. (1999). *J. Solid State Chem.* **144**, 209–215.
Wang, E., Greenblatt, M., Rachidi, E. I., Canadell, E., Whangbo, M. H. & Vadlamannati, S. (1989). *Phys. Rev. B*, **39**, 12969–12972.
Wang, S. L., Wang, C. C. & Lii, K. H. (1989). *J. Solid State Chem.* **82**, 298–302.
Whangbo, M. M., Canadell, E., Foury, P. & Pouget, J. P. (1991). *Science*, **252**, 96–98.
Witkowski, N., Garnier, M., Purdie, D., Baer, Y., Malterre, D. & Groult, D. (1997). *Solid State Commun.* **103**, 471–475.
Woodward, P. M., Sleight, A. W. & Vogt, T. (1995). *J. Phys. Chem. Solids*, **56**, 1305–1315.
Woodward, P. M., Sleight, A. W. & Vogt, T. (1997). *J. Solid State Chem.* **131**, 9–17.
d'Yachenko, O. G., Tabachenko, V. V. & Sundberg, M. (1995). *J. Solid State Chem.* **119**, 8–12.
Yan, Y., Kleman, M., Le Touze, C., Marcus, J., Schlenker, C. & Buffat, A. (1995). *Europhys. Lett.* **30**, 49–54.